Three-dimensional morphometric properties of rod and plate trabeculae in adolescent cancellous bone

Ding, Ming; Lin, Xiaozhe; Liu, Wenge

Published in:
Journal of Orthopaedic Translation

DOI:
10.1016/j.jot.2017.10.001

Publication date:
2018

Document version
Publisher's PDF, also known as Version of record

Journal of Orthopaedic Translation (2018) 12, 26–35

Available online at www.sciencedirect.com

ScienceDirect

journal homepage: http://ees.elsevier.com/jot

ORIGINAL ARTICLE

Three-dimensional morphometric properties of rod- and plate-like trabeculae in adolescent cancellous bone

Ming Ding [a,*], **Xiaozhe Lin** [b], **Wenge Liu** [c]

[a] *Orthopaedic Research Laboratory, Department of Orthopaedic Surgery and Traumatology, Odense University Hospital, Department of Clinical Research, University of Southern Denmark, 5000 Odense C, Denmark*
[b] *Department of Orthopedics, The Affiliated Fujian Provincial Jiguan Hospital of Fujian Health College, Fuzhou, Fujian 350001, PR China*
[c] *Department of Orthopedics, The Affiliated Union Hospital of Fujian Medical University, Fuzhou 350001, PR China*

Received 8 August 2017; received in revised form 2 October 2017; accepted 6 October 2017
Available online 13 November 2017

KEYWORDS
Adolescence;
Microarchitectural properties;
Trabecular plate;
Trabecular rod;
Volumetric spatial decomposition

Summary *Background/Objective:* Despite many researches have been carried out on the three-dimensional microarchitecture of cancellous bone, the morphometric properties of rod and plate trabeculae in adolescent cancellous bone have not yet been investigated. This study aimed to investigate three-dimensional morphometric properties of rod- and plate-like trabeculae in normal adolescent cancellous bone, and to compare them with adult cancellous bones to reveal morphometric changes from adolescence to adult life to obtain more insight into the subchondral bone adaptations during development and growth.
Methods: This study included 23 normal human proximal tibiae. These tibiae were divided into three groups: adolescents (9–17 years, n = 6), young adults (18–24 years, n = 9), and adults (25–30 years, n = 8). From each tibia, six cubic cancellous bone samples (dimensions $8 \times 8 \times 8$ mm^3) were sawed from each medial and lateral condyle, yielding a total of 276 samples. These samples were scanned using micro computed tomography leading to three-dimensional cubic voxel sizes of $10.5 \times 10.5 \times 10.5$ μm^3. The morphometric parameters of individual rod- and plate-like trabeculae were calculated and compared among three age groups.
Results: Significant differences in some morphometric parameters were revealed. The mean longitudinal length of rods was significantly greater in the adolescents than in the young adults. Plate volume density showed an increasing trend with age, although not significant. Trabeculae were more plate-like in adolescents in the medial condyle of adolescents than in the lateral condyle, and changed towards more plate-like trabeculae in the adults. The single best predictor for the mechanical properties was apparent density. Apparent density alone

* Corresponding author. Orthopaedic Research Laboratory, Department of Orthopaedic Surgery and Traumatology, Odense University Hospital, J.B. Winsloewsvej 15, 3rd floor, DK-5000 Odense C, Denmark.
E-mail address: ming.ding@rsyd.dk (M. Ding).

https://doi.org/10.1016/j.jot.2017.10.001

explained 59% variations in Young's modulus, 77% in ultimate stress and 34% in failure energy, respectively (all $p < 0.01$). Morphometric parameters might improve this prediction.
Conclusion: In conclusion, this study has reported for the first time the morphometric parameters of rod- and plate-like trabeculae in adolescent proximal tibial cancellous bone, which will improve our understanding of morphometric changes in individual trabeculae during development and growth. Furthermore, separate analysis of individual rods and plates may also help reveal disease-related morphometric changes beyond bone mineral density.
The translational potential of this article: A thorough quantification of individual trabeculae during development and growth may help understand disease-related 3-D morphometric changes beyond bone mineral density.

Introduction

Three-dimensional (3D) microarchitectural, mechanical, collagen and mineral properties of normal adolescent cancellous bone have been investigated to obtain more insight into the subchondral bone adaptations during development and growth [1]. Microcomputed tomography (micro-CT) imaging with high spatial resolution has enabled a global analysis of the sophisticated 3D microarchitecture of cancellous bone describing the average structure for the whole bone specimen in an unbiased and assumption-free manner. Specifically, model-independent measures of the trabecular microarchitecture such as volume fraction, connectivity density, degree of anisotropy, trabecular thickness, separation, surface density and type of the structure (rod or plate) have been standardized and routinized for the study of cancellous bone and provided a strong tool and new insights into the transformation of cancellous bone structure in diseases [2,3]. These investigations have revealed subchondral bone changes in proximal tibiae from development and growth to ageing [1,2] and disease-related changes such as osteoporosis [4], osteoarthritis [5,6], or diabetes [5].

With further advance of imaging techniques in recent years, the developments in software for micro-CT data sets have achieved the ability to analyse individual trabecular elements separately [7]. Volumetric spatial decomposition (VSD) of trabeculae, developed by Stauber and Müller [7], has enabled measurements of trabecular bone samples into its basic elements (rods and plates), which is a framework for the element-based description of bone morphometry. This technique has been applied to human cancellous bones from spinal column [8,9] and femoral heads [9]. The 3D microarchitecture and morphometry of rod- and plate-like trabeculae were quantified and related to Young's moduli as assessed by the experimental uniaxial compression test and computational finite element analysis [8]. It is concluded that the individual morphometry of rod- and plate-like trabeculae helps improving our understanding of the relative importance of structural changes in the determination of the stiffness of bone.

The combination of morphometric parameters of rod- and plate-like trabeculae and 3D microarchitecture is a useful tool for a detailed and quantitative description of age- and disease-related changes in the bone microarchitecture [9–11]. This methodology has enabled to show age-related and site differences in measures of individual trabeculae that may improve the understanding of the site-specific role of the bone microarchitecture in determining bone quality [8].

We have recently reported global microarchitectural properties of normal human adolescent cancellous bone and their physical properties, collagen and mineral and mechanical properties [1]. This study has revealed that adolescent cancellous bone has similar bone volume fraction, structure type and connectivity, and significantly lower tissue density, bone surface density and mineral concentration but higher collagen concentration than in the young adult and adult cancellous bones [1]. However, the morphometric properties of rod- and plate-like trabeculae in adolescent cancellous bone have not yet been investigated.

Thus, the aims of this study were to investigate 3D morphometric properties of rod- and plate-like trabeculae in normal adolescent cancellous bone and to compare them with adult cancellous bones to reveal morphometric changes from adolescence to adult life to obtain more insight into the subchondral bone adaptations during development and growth. We further evaluated the associations between the morphometric properties of rod- and plate-like trabeculae and their mechanical properties, and determined the best predictors for mechanical properties from the measured morphometric parameters, together with the 3D microarchitectural parameters and physical and compositional properties (i.e., densities, mineral and collagen concentrations) in a study [1], thus providing more insight into the adolescent bone microarchitecture and its role in determining mechanical properties. This investigation will improve our understanding of morphometric changes in individual rod- and plate-like trabeculae during development and growth. Prospectively, it may also help predict disease-related morphometric changes, such as osteoporosis-related fractures beyond bone mineral density, and effects of pharmaceutical intervention and osteoarthritis-related microdamages of subchondral bone.

We hypothesized that local morphometric parameters of the adolescent cancellous bone might be significantly different from those of adult cancellous bones, and the combination of 3D microarchitectural properties and morphometric parameters of individual rod- and plate-like

trabeculae could improve the prediction of mechanical properties.

Materials and methods

The materials used in this study have been described in detail by Ding et al [1]. Briefly, human left proximal tibiae were collected from 23 donors with mean age 21 years (9—30 years). All these donors were Caucasians, and 5 were females and 18 were males. A criterion for sample selection was strictly controlled [12], i.e., these donors had all died suddenly from either traumatic or acute disease. No history of musculoskeletal diseases was recorded. They had always been active physically and had no more than 2 weeks of immobilization before death. No macroscopic pathological changes were observed in tibiae, and the cartilage was intact. The protocol was approved by the Department of Orthopaedics and Institute of Forensic Medicine, Aarhus University Hospital, Denmark [1].

Specimen preparation

The processing of subchondral bone samples is described elsewhere [1]. These samples were harvested from the epiphyseal areas beneath a thin layer of the subchondral plate and above the growth plate. The specimens were sawed out from standardized locations of both condyles (EXAKT Diamond saw, Nordenstedt, Germany, and LEICA SP 1600 saw microtome, Wetzlar, Germany). These specimens had dimensions of $8 \times 8 \times 8$ mm^3 with identifiable orientations of anterior—posterior (AP), medial—lateral (ML) and cephalocaudal (CC) directions (Fig. 1). The orientations of samples were marked. After completing the preparation, the specimens were frozen and stored in sealed plastic

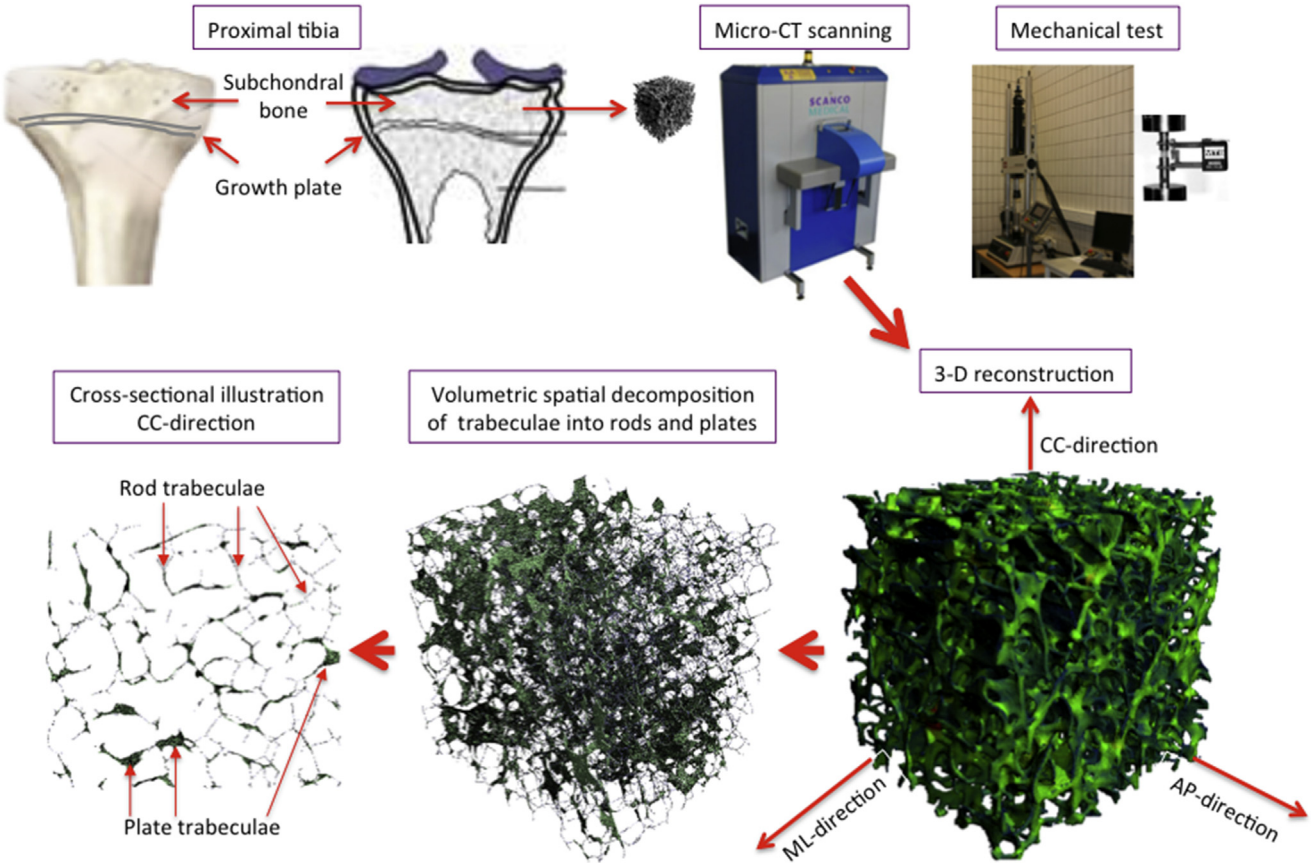

Figure 1 Study design. Cancellous bone samples were obtained beneath the thin layer of the subchondral plate and above the growth plate by using plastic template, which was available in different scales [1]. Four cubic specimens with dimensions of $8 \times 8 \times 8$ mm^3 were sawed out, two from each medial and lateral condyles of each 23 human normal proximal tibia. Three-dimensional reconstruction of cancellous bone is displayed at the right side of lower corner, and volumetric spatial decomposition of trabeculae is illustrated at the middle and left sides of lower panel. Orientations of the sample are indicated. To investigate possible differences, the samples were divided into three groups: adolescents (9—17 years), young adults (18—24 years) and adults (25—30 years). These samples were scanned using micro-CT, and volumetric spatial decomposition was performed to quantify rod- and plate-like trabeculae and related properties. Stepwise multiple linear regressions were performed to determine the best predictor for mechanical properties as dependent variables, and all measured global microarchitectural properties, local morphometric properties and physical and compositional properties as independent (explanatory) variables. Regression analyses were further performed to determine the best predictor for mechanical properties independent of bone mineral density. AP = anterior—posterior; CC = cephalocaudal; CT = computed tomography; ML = medial—lateral.

tubes at −20°C. Six samples from the standardized location of each medial and lateral condyle, i.e., a total 276 samples, were used in this study [1].

Micro-CT scanning

All 276 bone samples were scanned using micro-CT by means of a high-resolution scanner (vivaCT 40, Scanco Medical AG, Brüttisellen, Switzerland) to quantify their 3D micro-architectural properties. The 3D reconstruction cubic voxel sizes of the scanned images were 10.5 × 10.5 × 10.5 μm^3 (2048 × 2048 × 2048 pixels) with 32-bit grey levels. After scanning, the micro-CT images were segmented using the segmentation techniques [13] with a slight modification [14] to obtain accurate 3D imaging data sets (Fig. 1).

Three-dimensional cancellous bone microarchitecture

Three-dimensional microarchitectural parameters of adolescent cancellous bone were calculated [1]. These 3D microarchitectural parameters were bone volume fraction (BV/TV, %), structure model index (SMI), trabecular thickness (Tb.Th, μm), degree of anisotropy (DA, -), connectivity density (Conn.D, mm^{-3}), bone surface density (BS/TV, mm^{-1}), bone surface to volume ratio (BS/BV, mm^{-1}), trabecular separation (μm) and trabecular number (mm^{-1}), respectively [1]. These parameters have been reported in detail elsewhere [1] and are used in this study only in a regression model associated with mechanical, physical and compositional properties and local morphometric parameters (Fig. 1).

Morphometry of rod- and plate-like trabeculae

VSD of trabecular structures was performed using the techniques developed by Stauber and Müller [7] and Stauber et al [8] to compute local morphometric indices at a trabecular level. Morphometric parameters of individual rods and plates were quantified directly from 3D images (Fig. 1). All the parameters were computed by means of standard morphometric algorithms as implemented in the image processing language (Version 6.0; Scanco Medical AG, Switzerland). Each VSD analysis of a bone sample took approximately 8 hours. Basically, the following abbreviations are used as suggested by Stauber and Müller [7]: prefix Pl for plates, Ro for rods and El for elements (either plate or rod). V, S and Th are used to denote the volume, surface and thickness of one single element, and BV and BS for the sum of the volume and surface over all elements, respectively, and brackets (⟨⟩) to denote mean values averaged over all elements of the same type [7,8].

These local morphometric parameters, the measures of individual trabecular elements, were calculated. These parameters were the rod volume density (Ro.BV/TV) defined as the total rod volume divided by total volume of interest in percent, the plate volume density (Pl.BV/TV) defined as total plate volume divided by total volume of interest in percent, the relative bone volume fraction of rods (Ro.BV/BV) and plates (Pl.BV/BV = 100% − Ro.BV/BV) in percentage, were determined as well [7]. Furthermore, the mean volume (⟨Ro.V⟩, ⟨Pl.V⟩), the mean surface (⟨Ro.S⟩, ⟨Pl.S⟩) and the mean thickness (⟨Ro.Th⟩, ⟨Pl.Th⟩) averaged for each structure over all rods and plates separately were calculated. The mean orientation (⟨Ro.θ⟩), the angle between the orientation of the element and the image axis that aligned along the CC direction of the tibia, and the mean longitudinal length of trabecula (⟨Ro.Le⟩, ⟨Pl.Le⟩) were computed (Table 1, Fig. 1) [7,8].

Mechanical properties and collagen and mineral concentrations

After micro-CT scanning, four samples from each medial and lateral condyle (i.e., two anterior and two posterior samples, and left two middle for another study) were used for the mechanical test [1]. These samples (n = 184) were tested in compression on an 858 Bionix MTS hydraulic material testing system (MTS Systems Co., Minneapolis, Minnesota, USA), using a 1 kN load cell. The mechanical tests were performed destructively in the CC direction to determine ultimate stress (strength, MPa), Young's modulus (MPa), failure energy (kJ/cm^3) and ultimate strain (%) [1]. These parameters were only used in a regression model associated with 3D microarchitectural properties and morphometric parameters of rod- and plate-like trabeculae [1].

Furthermore, bone densities and mineral and collagen concentrations were determined as described in detail elsewhere [12], and the methods are briefly reported subsequently. After defatting in a 1:1 mixture of alcohol and acetone for 48 hours, the specimens were heated in a Ringer's solution at 60—65°C for about 1 hours. After cooling, trypsin from porcine pancreas (Sigma—Aldrich) was added to 0.5% and the specimens were incubated for 16 hour at 37°C. The dry weight of the freeze-dried specimens and the submerged weight of the specimens were recorded using a Mettler AT250 balance (Mettler Instruments AG, Greifensee, Switzerland). Apparent density (g/cm^3) was calculated as dry weight of the defatted specimen per total volume of the specimen, and tissue density (g/cm^3) was calculated as dry weight of the defatted specimen per volume of the bone matrix excluding marrow space [12].

Finally, the specimens were further cut into four pieces for duplicate determinations of mineral (ash) and collagen concentrations. The collagen (tissue) concentration was determined as collagen weight of the specimen per dry weight of the specimen (%). The specimens were burned in a muffled oven at 100°C for 2 hours and 580° for 18 hours, and the dry weight of the ash was recorded. The mineral concentration was determined as the mineral weight (ash weight) of the specimen per dry weight of the specimen (%) [14,20]. These parameters were also only used in a regression model associated with microarchitectural properties and individual trabecular morphometric parameters [1].

Statistical analysis

All statistical analyses were done using IBM SPSS (version 24; SPSS Inc, Chicago, Illinois).

The differences between properties in three age groups were compared by a one-way analysis of variance, and the

Table 1 Comparison of rod- and plate-like trabeculae of proximal tibial condyles among three age groups (mean ± SD, 276 samples from n = 23 tibiae).

Local morphometry	Adolescents (g1, 9–17 y, n = 6)	Young adults (g2, 18–24 y, n = 9)	Adults (g3, 25–30 y, n = 8)	One-way ANOVA for three groups	Difference between groups
Ro.BV/TV (%)	4.18 ± 1.48	3.96 ± 1.16	4.13 ± 0.86	p = 0.926	
Pl.BV/TV (%)	15.84 ± 3.36	17.30 ± 3.70	18.93 ± 1.38	p = 0.182	
Ro.BV/BV (%)	23.5 ± 9.1	22.6 ± 8.8	20.5 ± 3.48	p = 0.714	
Pl.BV/BV (%)	76.5 ± 9.1	77.4 ± 8.8	79.5 ± 3.5	p = 0.714	
⟨Ro.V⟩ (10^3 μm^3)	4.33 ± 0.73	3.57 ± 1.42	4.14 ± 0.80	p = 0.302	
⟨Ro.S⟩ (10^3 μm^2)	190.1 ± 20.9	157.6 ± 40.7	181.1 ± 27.3	p = 0.146	
⟨Ro.Th⟩ (μm)	82.1 ± 5.9	72.6 ± 8.7	81.0 ± 7.7	p = 0.043	
⟨Ro.θ⟩ (rad)	59.0 ± 0.54	60.1 ± 1.00	58.4 ± 1.36	p = 0.013	g2 > g3
⟨Ro.Le⟩ (μm)	212.6 ± 18.7	173.9 ± 29.4	195.2 ± 24.3	p = 0.027	g1 > g2
⟨Pl.V⟩ (10^3 μm^3)	31.9 ± 10.6	23.8 ± 13.7	37.3 ± 18.6	p = 0.199	
⟨Pl.S⟩ (10^3 μm^2)	757.7 ± 215.7	600.2 ± 317.0	865.2 ± 358.1	p = 0.234	
⟨Pl.Th⟩ (μm)	70.9 ± 4.1	63.4 ± 7.7	74.5 ± 17.3	p = 0.156	
⟨Pl.θ⟩ (rad)	62.0 ± 2.7	61.9 ± 1.4	63.0 ± 0.6	p = 0.356	
⟨Pl.Le⟩ (μm)	217.7 ± 35.9	179.0 ± 46.2	222.1 ± 62.9	p = 0.187	

Pl.BV/BV = relative bone volume fraction of plates; Pl.BV/TV = plate volume density; ⟨Pl.Le⟩ = mean longitudinal length of plates; ⟨Pl.S⟩ = mean surface of plates; ⟨Pl.Th⟩ = mean thickness of plates; ⟨Pl.V⟩ = mean volume of plates; ⟨Pl.θ⟩ = mean orientation of plates; Ro.BV/BV = relative bone volume fraction of rods; Ro.BV/TV = rod volume density; ⟨Ro.Le⟩ = mean longitudinal length of rods; ⟨Ro.S⟩ = mean surface of rods; ⟨Ro.Th⟩ = mean thickness of rods; ⟨Ro.V⟩ = mean volume of rods; ⟨Ro.θ⟩ = mean orientation of rods.

differences between medial and lateral condyles were assessed by paired *t* test. The equal variance of the data was assessed by the Levene test and the normality by the Omnibus test. If the *F* test revealed a significant level, *post hoc* multiple comparisons were performed by the Bonferroni test or the Dunnett test when appropriate to test difference between groups. Furthermore, linear and stepwise multiple linear regression analyses were used to assess the associations between one of the mechanical properties as a dependent variable and all measured 3D microarchitectural properties and morphometric properties of rod- and plate-like trabeculae and physical and compositional properties as independent (explanatory) variables. A p value <0.05 was considered significant. Because there were only five females included, the potential gender-related variations could not be analysed.

Results

Three-dimensional reconstructions of micro-CT images of samples with different ages are displayed (Fig. 2). After VSD of trabecular elements, the mean orientation of rods relative to the image axis of a sample (i.e., the axial CC direction of tibia) was significantly greater in the young adult than in the adults. The mean longitudinal length of rods was significantly greater in the adolescents than in the young adults. Plate density showed an increasing trend with age, although not significant. The other measured parameters did not reach significant difference among groups (Table 1).

In the adolescents, the relative volume fraction of plates was significantly greater medially than laterally, and the rod volume density, relative bone volume fraction of rods and the mean longitudinal length of plates were lower medially than laterally. In the young adults, rod volume density was lower medially than laterally. In the adults, mean orientation of plates was greater medially than laterally (Table 2).

In the medial condyle, mean orientation of rods in the young adults was significantly greater than in the adults. In the lateral condyle, mean thickness of rods was lower in the young adults than in the adolescents and the adults, mean orientation of rods was greater in the young adults than in the adults and mean longitudinal length of rods was greater in the adolescents than in the young adults (Table 3).

The apparent density (g/cm^3) has been calculated [1], and is reported because it is a key parameter for determining mechanical properties. The adolescents have an overall value of 0.34 ± 0.08 (medial, 0.36 ± 0.08; lateral, 0.33 ± 0.08; p = 0.27), the young adults 0.37 ± 2.25 (medial, 0.37 ± 0.08; lateral, 0.37 ± 0.11; p = 0.79) and the adults 0.39 ± 0.09 (medial, 0.42 ± 0.08; lateral, 0.36 ± 0.09; p = 0.05) [1].

Stepwise multiple linear regression analyses were performed to determine the best predictors for mechanical properties. Apparent density alone explained 59% variation in Young's modulus ($p < 0.001$), 68% and 75% by adding plate thickness and rod volume density, respectively. Apparent density alone explained 77% variation in ultimate stress ($p < 0.001$), 83% and 89% by adding plate volume density and plate volume, respectively. Apparent density alone explained 34% variation in failure energy ($p < 0.01$) (Table 4).

In the adolescents, mean orientation of rods explained 71% variation in Young's modulus. Plate volume explained 81% variation in ultimate stress. ConnD explained 94% variation in failure energy, 99% by adding the mean orientation of rods. In the young adults, apparent density explained 79% variation in Young's modulus and 86% variation in ultimate stress. Bone volume fraction explained 67%

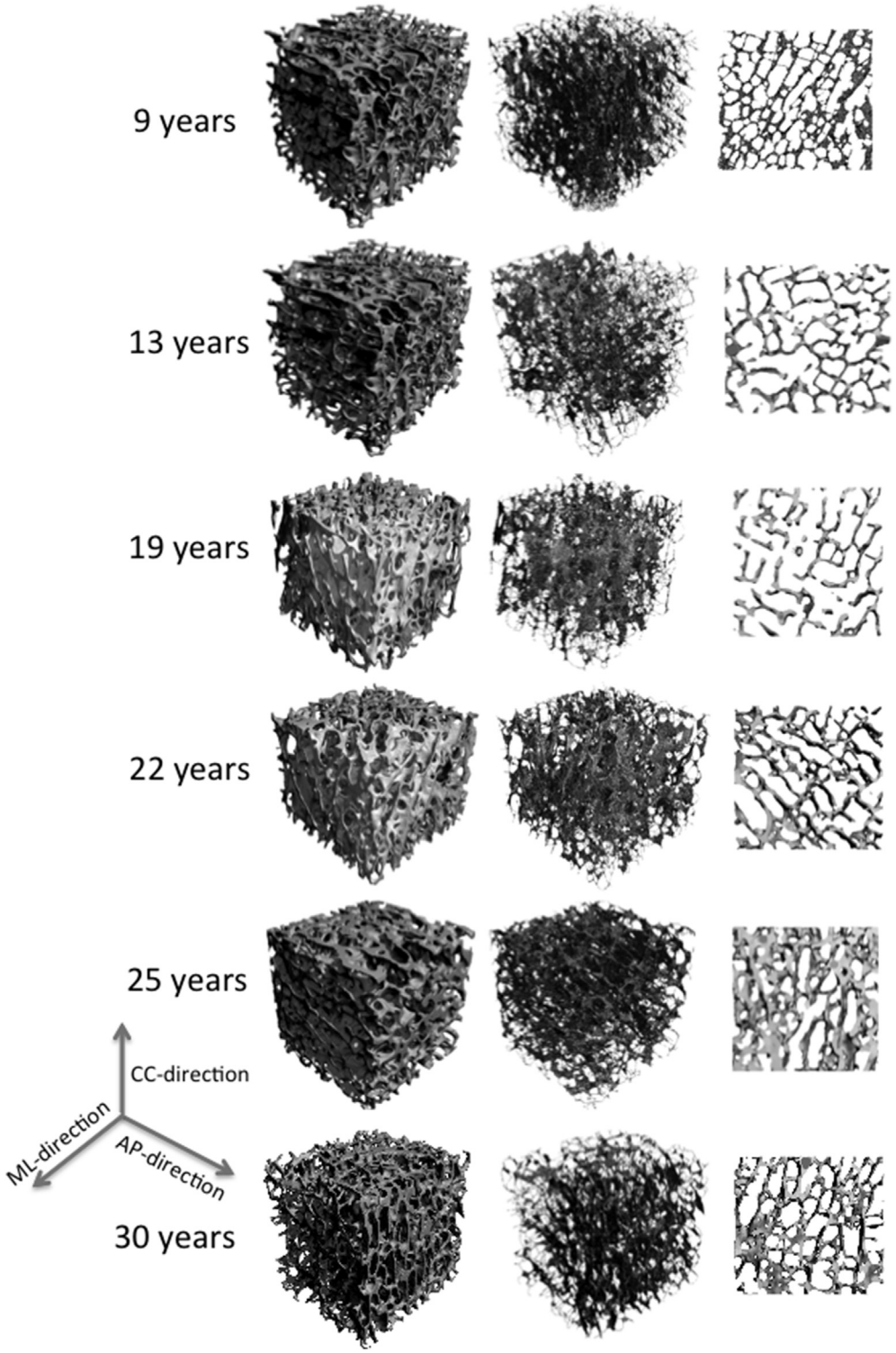

Figure 2 Three-dimensional reconstructions of micro-CT images for selected samples with different ages. Differences in the microarchitecture are illustrated in the panel (A), volumetric spatial decomposition of trabeculae is shown in the panel (B), with further focus on the three-dimensional reconstruction of 10 slices in the panel (C). Orientations of the sample are indicated. AP = anterior—posterior; CC = cephalocaudal; CT = computed tomography; ML = medial—lateral.

variation in failure energy, 83% by adding the collagen content. In the adults, bone surface density explained 83% variation in Young's modulus. Apparent density explained 76% variation in ultimate stress (Table 4).

Discussion

This study investigated the morphometric parameters of rod- and plate-like trabeculae in normal adolescent

Table 2 Comparison of rod- and plate-like trabeculae between the medial and the lateral tibial condyles (mean ± SD, 276 samples from n = 23 tibiae).

Local morphometry	Adolescents (g1, 9–17 y, n = 6)			Young adults (g2, 18–24 y, n = 9)			Adults (g3, 25–30 y, n = 8)		
	Medial	Lateral	Medial vs. lateral	Medial	Lateral	Medial vs. lateral	Medial	Lateral	Medial vs. lateral
Ro.BV/TV (%)	3.68 ± 1.45	4.69 ± 1.60	p = 0.019	3.70 ± 0.81	4.82 ± 1.80	p = 0.006	3.71 ± 1.18	4.49 ± 1.06	p = 0.067
Pl.BV/TV (%)	17.77 ± 4.45	13.90 ± 3.13	p = 0.053	18.46 ± 3.92	16.65 ± 7.58	p = 0.632	21.27 ± 4.67	16.30 ± 5.12	p = 0.095
Ro.BV/BV (%)	19.37 ± 9.66	27.42 ± 9.49	p = 0.014	18.43 ± 5.91	26.99 ± 13.9	p = 0.053	19.99 ± 6.58	24.79 ± 7.82	p = 0.050
Pl.BV/BV (%)	80.63 ± 9.66	72.58 ± 9.49	p = 0.014	81.57 ± 5.91	73.01 ± 13.9	p = 0.053	84.01 ± 6.58	75.21 ± 7.82	p = 0.050
⟨Ro.V⟩ (10^3 μm^3)	4.43 ± 0.85	4.43 ± 0.89	p = 0.988	3.52 ± 1.59	3.63 ± 1.33	p = 0.682	3.98 ± 0.93	4.31 ± 0.77	p = 0.172
⟨Ro.S⟩ (10^3 μm^2)	189.4 ± 25.1	190.7 ± 25.9	p = 0.920	155.6 ± 49.8	159.9 ± 34.9	p = 0.659	175.4 ± 32.8	186.9 ± 25.1	p = 0.151
⟨Ro.Th⟩ (μm)	81.7 ± 7.2	82.5 ± 6.8	p = 0.793	71.8 ± 1.1	73.5 ± 7.2	p = 0.547	79.0 ± 9.3	83.1 ± 7.3	p = 0.110
⟨Ro.θ⟩ (rad)	59.6 ± 0.87	58.5 ± 0.89	p = 0.112	60.3 ± 1.30	58.9 ± 0.90	p = 0.283	58.5 ± 1.4	58.3 ± 1.37	p = 0.492
⟨Ro.Le⟩ (μm)	205.4 ± 27.2	219.5 ± 21.7	p = 0.328	170.2 ± 39.9	177.9 ± 29.7	p = 0.565	182.6 ± 32.6	207.9 ± 26.3	p = 0.073
⟨Pl.V⟩ (10^3 μm^3)	27.3 ± 7.1	36.5 ± 16.5	p = 0.158	27.2 ± 20.1	20.4 ± 10.3	p = 0.252	35.1 ± 21.3	39.4 ± 19.9	p = 0.520
⟨Pl.S⟩ (10^3 μm^2)	623.3 ± 129.4	889.5 ± 365.4	p = 0.108	662.3 ± 458.8	539.4 ± 242.3	p = 0.350	800.9 ± 477.0	929.6 ± 383.4	p = 0.478
⟨Pl.Th⟩ (μm)	69.4 ± 5.8	72.4 ± 3.4	p = 0.177	62.9 ± 9.1	64.1 ± 7.7	p = 0.620	66.8 ± 5.5	82.3 ± 32.9	p = 0.215
⟨Pl.θ⟩ (rad)	62.2 ± 2.1	61.8 ± 3.3	p = 0.539	62.0 ± 2.5	61.8 ± 1.4	p = 0.833	63.9 ± 0.9	62.1 ± 1.2	p = 0.028
⟨Pl.Le⟩ (μm)	191.5 ± 47.2	243.3 ± 34.8	p = 0.024	172.0 ± 57.6	186.7 ± 0.57	p = 0.429	177.5 ± 36.9	266.6 ± 123.5	p = 0.098

Paired *t* tests were performed.

Pl.BV/BV = relative bone volume fraction of plates; Pl.BV/TV = plate volume density; ⟨Pl.Le⟩ = mean longitudinal length of plates; ⟨Pl.S⟩ = mean surface of plates; ⟨Pl.Th⟩ = mean thickness of plates; ⟨Pl.V⟩ = mean volume of plates; ⟨Pl.θ⟩ = mean orientation of plates; Ro.BV/BV = relative bone volume fraction of rods; Ro.BV/TV = rod volume density; ⟨Ro.Le⟩ = mean longitudinal length of rods; ⟨Ro.S⟩ = mean surface of rods; ⟨Ro.Th⟩ = mean thickness of rods; ⟨Ro.V⟩ = mean volume of rods; ⟨Ro.θ⟩ = mean orientation of rods.

Table 3 Comparison of rod- and plate-like trabeculae of the medial and the lateral tibial condyles among three groups (mean ± SD, 276 samples from n = 23 tibiae).

Local morphometry	Adolescents (g1, 9–17 y, n = 6)		Young adults (g2, 18–24 y, n = 9)		Adults (g3, 25–30 y, n = 8)		One-way ANOVA for medial condyle	Difference between groups	One-way ANOVA for lateral condyle	Difference between groups
	Medial	Lateral	Medial	Lateral	Medial	Lateral				
Ro.BV/TV (%)	3.68 ± 1.45	4.69 ± 1.60	3.70 ± 0.81	4.82 ± 1.80	3.71 ± 1.18	4.49 ± 1.06	p = 0.893		p = 0.960	
Pl.BV/TV (%)	17.77 ± 4.45	13.90 ± 3.13	18.46 ± 3.92	16.65 ± 7.58	21.27 ± 4.67	16.30 ± 5.12	p = 0.098		p = 0.582	
Ro.BV/BV (%)	19.37 ± 9.66	27.42 ± 9.49	18.43 ± 5.91	26.99 ± 13.9	19.99 ± 6.58	24.79 ± 7.82	p = 0.479		p = 0.943	
Pl.BV/BV (%)	80.63 ± 9.66	72.58 ± 9.49	81.57 ± 5.91	73.01 ± 13.9	84.01 ± 6.58	75.21 ± 7.82	p = 0.479		p = 0.943	
⟨Ro.V⟩ (10^3 μm^3)	4.43 ± 0.85	4.43 ± 0.89	3.52 ± 1.59	3.63 ± 1.33	3.98 ± 0.93	4.31 ± 0.77	p = 0.376		p = 0.285	
⟨Ro.S⟩ (10^3 μm^2)	189.4 ± 25.1	190.7 ± 25.9	155.6 ± 49.8	159.9 ± 34.9	175.4 ± 32.8	186.9 ± 25.1	p = 0.261		p = 0.095	
⟨Ro.Th⟩ (μm)	81.7 ± 7.2	82.5 ± 6.8	71.8 ± 1.1	73.5 ± 7.2	79.0 ± 9.3	83.1 ± 7.3	p = 0.141		p = 0.020	g2 < g1,g3
⟨Ro.θ⟩ (rad)	59.6 ± 0.87	58.5 ± 0.89	60.3 ± 1.30	58.9 ± 0.90	58.5 ± 1.4	58.3 ± 1.37	p = 0.029	g2 > g3	p = 0.014	g2 > g3
⟨Ro.Le⟩ (μm)	205.4 ± 27.2	219.5 ± 21.7	170.2 ± 39.9	177.9 ± 29.7	182.6 ± 32.6	207.9 ± 26.3	p = 0.178		p = 0.017	g1 > g2
⟨Pl.V⟩ (10^3 μm^3)	27.3 ± 7.1	36.5 ± 16.5	27.2 ± 20.1	20.4 ± 10.3	35.1 ± 21.3	39.4 ± 19.9	p = 0.622		p = 0.049	
⟨Pl.S⟩ (10^3 μm^2)	623.3 ± 129.4	889.5 ± 365.4	662.3 ± 458.8	539.4 ± 242.3	800.9 ± 477.0	929.6 ± 383.4	p = 0.685		p = 0.048	
⟨Pl.Th⟩ (μm)	69.4 ± 5.8	72.4 ± 3.4	62.9 ± 9.1	64.1 ± 7.7	66.8 ± 5.5	82.3 ± 32.9	p = 0.232		p = 0.202	
⟨Pl.θ⟩ (rad)	62.2 ± 2.1	61.8 ± 3.3	62.0 ± 2.5	61.8 ± 1.4	63.9 ± 0.9	62.1 ± 1.2	p = 0.134		p = 0.944	
⟨Pl.Le⟩ (μm)	191.5 ± 47.2	243.3 ± 34.8	172.0 ± 57.6	186.7 ± 0.57	177.5 ± 36.9	266.6 ± 123.5	p = 0.749		p = 0.140	

Paired *t* tests were performed.

ANOVA = analysis of variance; Pl.BV/BV = relative bone volume fraction of plates; Pl.BV/TV = plate volume density; ⟨Pl.Le⟩ = mean longitudinal length of plates; ⟨Pl.S⟩ = mean surface of plates; ⟨Pl.Th⟩ = mean thickness of plates; ⟨Pl.V⟩ = mean volume of plates; ⟨Pl.θ⟩ = mean orientation of plates; Ro.BV/BV = relative bone volume fraction of rods; Ro.BV/TV = rod volume density; ⟨Ro.Le⟩ = mean longitudinal length of rods; ⟨Ro.S⟩ = mean surface of rods; ⟨Ro.Th⟩ = mean thickness of rods; ⟨Ro.V⟩ = mean volume of rods; ⟨Ro.θ⟩ = mean orientation of rods.

Table 4 Stepwise multiple linear regression analysis on the associations between mechanical properties as dependent variables, and all measured global microarchitectural, local morphometric properties and physical and compositional properties as independent variables (all data, n = 23).

Mechanical properties	Young's modulus (MPa)	Ultimate stress (MPa)	Failure energy (kJ/cm^3)	Ultimate strain (%)
Regression analysis based on entire data				
First variable was entered into the equation (R^2)	Apparent density (0.59)**	Apparent density (0.77)**	Apparent density (0.34)*	No variables were entered into the equation
Second variable was added (R^2)	Plate thickness (0.68)**	Plate volume density (0.83)**		
Third variable was added (R^2)	Rod volume density (0.75)**	Plate volume (0.89)**		
Regression analysis based on adolescent data only				
First variable was entered into the equation (R^2)	Ro.θ (0.71)**	Plate volume (0.81)**	Connectivity density (0.94)**	No variables were entered into the equation
Second variable was added (R^2)			Rod θ (0.99)**	
Third variable was added (R^2)				
Regression analysis based on young adult data only				
First variable was entered into the equation (R^2)	Apparent density (0.79)**	Apparent density (0.86)**	Bone volume fraction (0.67)**	No variables were entered into the equation
Second variable was added (R^2)			Collagen content (0.83)**	
Third variable was added (R^2)				
Regression analysis based on adult data only				
First variable was entered into the equation (R^2)	Bone surface density (0.83)**	Apparent density (0.76)**	No variables were entered into the equation	No variables were entered into the equation
Second variable was added (R^2)				
Third variable was added (R^2)				

*$p < 0.01$
**$p < 0.001$.

cancellous bone in proximal tibiae and compared with the young adults and the adults. This study further determined the best predictors for mechanical properties from the measured morphometric parameters of individual rod- and plate-like trabeculae together with 3D microarchitectural properties and physical and compositional properties in an early study [1]. The present study revealed significant differences in some morphometric parameters among three age groups and between condyles. The single best predictor for the mechanical properties except ultimate strain was apparent density. Adding morphometric parameters would improve this prediction.

Using a new approach of VSD of trabeculae from micro-CT images, a 3D bone structure was divided into its basic rod and plate elements. This approach was based on an image skeletonization method, where two model parameters were used to identify an ideal skeleton, and various parameters of the local morphometric index can be computed. A previous study has shown that local morphometric indices are reliable measures and could demonstrate large differences between samples. Morphometric analysis of rod- and plate-like trabeculae has provided insight into structural differences of the cancellous bone in a local individual trabecular fashion [7].

This study showed that differences among three groups were particularly significant in the mean orientation of rods relative to the image axis with greater in the young adults than in the adults, and also significant in the mean longitudinal length of rod with lowest value in the young adults (Table 1). Specifically, the mean orientation of rods relative to the image axis increased from adolescents to the greatest values in the young adults, and then declined in the adults. The mean longitudinal length of rods decreased from adolescents to be lowest in the young adults and then increased in the adults. Plate volume density showed an increasing trend with age, although not significant. The trend of plate volume density was similar to the observed trend in the SMI [1], suggesting trabeculae changed towards more plate-like structure from adolescents to adults. These results were in line with a previous report that trabeculae in young to middle ages were more plate-like structures [15]. Other measured parameters were relatively constant and did not differ from adolescents to adults (Table 1). These results revealed the particular active morphometric parameters that changed from development to growth and during bone modelling and remodelling.

A previous publication has shown the differences in microarchitecture between medial and lateral condyles. In the medial condyle, bone surface density was significantly lower in the adolescents than in the adults, with significantly greater trabecular separation and lower trabecular number in the adolescents compared with the young adults and the adults [1]. The TbTh in the adolescents was significantly greater than in the young adults, with

significantly greater anisotropy in the young adults than in the adolescents and the adults, whereas the lateral condyle did not show microarchitectural differences among the groups [1]. Some morphometric parameters measured between the medial and lateral condyles also differ from each other in the three age groups (Table 2). In the adolescents, the medial condyle had relatively greater plate volume density (not significant) and significantly greater relative volume fraction of plates, and lower relative bone volume fraction of rods than the lateral condyles. These results are in line with the greater SMI that trabeculae at the medial condyle are more plate-like structures, which might be because of the fact that the medial condyle of tibiae receives more force during daily loading. In the young adults and the adults, the medial condyle had lower rod volume density than the lateral condyle, suggesting a clear trend of microarchitectural changes during growth, so that the lateral trabeculae were more rod-like structures, whereas trabeculae in the medial condyle were more plate-like structures [1] (Table 2). Some differences were seen after separate analysis of morphometric properties between the medial and the lateral condyle over the three age groups (Table 3). These changes should be considered together with the other morphometric parameters.

Taken together, the present study has demonstrated local morphometric changes during development and growth. In particular, the mean longitudinal length of rods was significantly greater in the adolescent than in the young adult. Plate volume density showed an increasing trend with age, although not significant. It is revealed that trabeculae were more plate-like structures in adolescents in the medial condyle than in the lateral condyle and changed towards more plate-like structures in the adults.

The analysis of the associations between morphometric parameters and mechanical properties revealed that Young's modulus and ultimate stress correlated best with plate volume density ($R = 0.66$, $R = 0.79$, respectively). These results supported a previous assumption that plate-like trabeculae reflected stronger mechanical properties [15] in the uniaxial loading direction. Failure energy significantly correlated with plate volume density ($R = 0.57$) and plate volume ($R = 0.44$). Thus, plate properties like plate volume density are better relevant trabecular morphometric parameters correlated with mechanical properties.

This study determined the best predictors (Table 4) for mechanical properties by means of a stepwise multiple linear regression analysis. In the analysis, the mechanical properties represent dependent variables, and all the measured 3D microarchitectural properties and morphometric parameters of rod- and plate-like trabeculae and physical and compositional properties represent independent variables. The apparent density appears to be the single best predictor for mechanical properties apart from ultimate strain. These results are in line with previous studies [8,12]. The morphometric parameters will improve this prediction (Table 4). Furthermore, a stepwise multiple linear regression analysis is reported here when data are divided into three age groups. However, care must be taken because the sample size becomes small.

Three-dimensional microarchitectural analysis of trabecular bone has been a classical method for the quantification of cancellous bone microarchitecture. Recently, several attempts have been made to quantify individual morphometric parameters by decomposing trabeculae into rod and plate elements [7,11,16–20]. Stauber and Müller [7] proposed a computational approach for the VSD of trabecular structures into its basic rod and plate elements. This method has been validated and demonstrated the importance of local morphometry in assessing bone mechanical properties [8], vertebral bone strength [10] and in understanding age-related changes in the local bone microstructure [9]. Other researchers have also developed similar techniques. Van Ruijven et al [21] reported the effect of bone loss on rod-like and plate-like trabeculae in mandibular condyle. Guo's group has developed a technique called individual trabecular segmentation, to assess trabecular plate and rod microstructure separately based on micro-CT images [11], and related to mechanical properties [22] and tissue mineral density [23]. They have applied this technique to quantify local morphometric changes in *in vivo* from high-resolution peripheral quantitative CT measurements at both the radius and tibia in patients with postmenopausal vertebral fractures [18]. They also used this technique to discriminate postmenopausal fragility fractures [18,19], and postmenopausal women with vertebral fractures [24] or treated with glucocorticoids [25].

With this advanced technique, morphometric analysis of individual trabeculae will undoubtedly play an important role in quantifying individual trabecular morphometry of cancellous bone. This technique will provide more insight into the mechanism of microarchitectural changes during ageing, fracture repair, bone regeneration, disease processes and the effects of pharmaceutical intervention beyond bone density.

Several limitations of this study need to be mentioned. First, a relatively limited number of samples were used in this study that comprise the general conclusions, and any interpretation from this data set should be of caution. The real association between mechanical and 3D microarchitectural properties and morphometric parameters of rod- and plate-like trabeculae should be confirmed using large data set. Second, the samples were harvested from proximal tibiae, and the properties may vary between anatomic locations, and, e.g., the properties at lumbar spine and femoral head may have substantial differences from tibiae. Nevertheless, this study is unique as it is the first report, to the best of our knowledge, which describes the individual morphometric parameters of rod- and plate-like trabeculae and its roles in predicting mechanical properties, and the associations among various properties in adolescent cancellous bone.

Conclusions

This study has revealed for the first time the morphometric parameters of rod- and plate-like trabeculae in adolescent cancellous bone in the proximal tibiae and compared with the young adults and adults. The present study demonstrated that significant differences in some morphometric parameters, e.g., the mean orientation of rods relative to the image axis, were significantly greater

in the young adults than in the adults. Plate volume density showed an increasing trend with age, although not significant. Trabeculae in the medial condyle were more plate-like structures in adolescents and changed towards more plate-like structures in the adults. The single best predictor for the mechanical properties was apparent density. Morphometric parameters might improve this prediction. This study will improve our understanding of morphometric changes in individual trabeculae during development and growth. Furthermore, separate analysis of individual rods and plates may also further quantify disease-related morphometric changes beyond bone mineral density.

Conflicts of interest

The authors have no conflicts of interest to report.

Acknowledgements/Funding

We thank Dr. Martin Stauber, Scanco Medical AG., Brüttisellen, Switzerland for technical help of VSD software, and Gitte H. Reinberg for technical assistance. This study is kindly supported by the Region of Southern Denmark Research Funding (08/17871 & 15/24851, MD) and the Danish Health Research Council (SSVF22-04-0705, MD). We thank Professor Ivan Hvid for providing tibial samples.

References

[1] Ding M, Danielsen CC, Hvid I, Overgaard S. Three-dimensional microarchitecture of adolescent cancellous bone. Bone 2012;51:953—60.
[2] Ding M. Microarchitectural adaptations in aging and osteoarthrotic subchondral bone issues. Acta Orthop Suppl 2010;81:1—53.
[3] Odgaard A. Three-dimensional methods for quantification of cancellous bone architecture. Bone 1997;20:315—28.
[4] Dequeker J, Aerssens J, Luyten FP. Osteoarthritis and osteoporosis: clinical and research evidence of inverse relationship. Aging Clin Exp Res 2003;15:426—39.
[5] Wen CY, Chen Y, Tang HL, Yan CH, Lu WW, Chiu KY. Bone loss at subchondral plate in knee osteoarthritis patients with hypertension and type 2 diabetes mellitus. Osteoarthr Cartil 2013;21:1716—23.
[6] Roberts BC, Thewlis D, Solomon LB, Mercer G, Reynolds KJ, Perilli E. Systematic mapping of the subchondral bone 3D microarchitecture in the human tibial plateau: variations with joint alignment. J Orthop Res 2017;35:1927—41.
[7] Stauber M, Müller R. Volumetric spatial decomposition of trabecular bone into rods and plates—a new method for local bone morphometry. Bone 2006;38:475—84.
[8] Stauber M, Rapillard L, van Lenthe GH, Zysset P, Muller R. Importance of individual rods and plates in the assessment of bone quality and their contribution to bone stiffness. J Bone Min Res 2006;21:586—95.
[9] Stauber M, Muller R. Age-related changes in trabecular bone microstructures: global and local morphometry. Osteoporos Int 2006;17:616—26.
[10] Parkinson IH, Badiei A, Stauber M, Codrington J, Muller R, Fazzalari NL. Vertebral body bone strength: the contribution of individual trabecular element morphology. Osteoporos Int 2012;23:1957—65.
[11] Liu XS, Sajda P, Saha PK, Wehrli FW, Bevill G, Keaveny TM, et al. Complete volumetric decomposition of individual trabecular plates and rods and its morphological correlations with anisotropic elastic moduli in human trabecular bone. J Bone Min Res 2008;23:223—35.
[12] Ding M, Dalstra M, Danielsen CC, Kabel J, Hvid I, Linde F. Age variations in the properties of human tibial trabecular bone. J Bone Jt Surg Br 1997;79:995—1002.
[13] Ding M, Odgaard A, Hvid I. Accuracy of cancellous bone volume fraction measured by micro-CT scanning. J Biomech 1999;32:323—6.
[14] Ding M, Danielsen CC, Hvid I. Age-related three-dimensional microarchitectural adaptations of subchondral bone tissues in Guinea pig primary osteoarthrosis. Calcif Tissue Int 2006;78:113—22.
[15] Ding M, Hvid I. Quantification of age-related changes in the structure model type and trabecular thickness of human tibial cancellous bone. Bone 2000;26:291—5.
[16] Pothuaud L, Porion P, Lespessailles E, Benhamou CL, Levitz P. A new method for three-dimensional skeleton graph analysis of porous media: application to trabecular bone microarchitecture. J Microsc 2000;199:149—61.
[17] Pothuaud L, Laib A, Levitz P, Benhamou CL, Majumdar S. Three-dimensional-line skeleton graph analysis of high-resolution magnetic resonance images: a validation study from 34-microm-resolution microcomputed tomography. J Bone Min Res 2002;17:1883—95.
[18] Liu XS, Wang J, Zhou B, Stein E, Shi X, Adams M, et al. Fast trabecular bone strength predictions of HR-pQCT and individual trabeculae segmentation-based plate and rod finite element model discriminate postmenopausal vertebral fractures. J Bone Min Res 2013;28:1666—78.
[19] Liu XS, Stein EM, Zhou B, Zhang CA, Nickolas TL, Cohen A, et al. Individual trabecula segmentation (ITS)-based morphological analyses and microfinite element analysis of HR-pQCT images discriminate postmenopausal fragility fractures independent of DXA measurements. J Bone Min Res 2012;27:263—72.
[20] Stauber M, Muller R. A sensitivity analysis of the volumetric spatial decomposition algorithm. Comput Methods Biomech Biomed Eng 2007;10:25—37.
[21] van Ruijven LJ, Giesen EB, Mulder L, Farella M, van Eijden TM. The effect of bone loss on rod-like and plate-like trabeculae in the cancellous bone of the mandibular condyle. Bone 2005;36:1078—85.
[22] Wang J, Zhou B, Liu XS, Fields AJ, Sanyal A, Shi X, et al. Trabecular plates and rods determine elastic modulus and yield strength of human trabecular bone. Bone 2015;72:71—80.
[23] Wang J, Kazakia GJ, Zhou B, Shi XT, Guo XE. Distinct tissue mineral density in plate- and rod-like trabeculae of human trabecular bone. J Bone Min Res 2015;30:1641—50.
[24] Wang J, Stein EM, Zhou B, Nishiyama KK, Yu YE, Shane E, et al. Deterioration of trabecular plate-rod and cortical microarchitecture and reduced bone stiffness at distal radius and tibia in postmenopausal women with vertebral fractures. Bone 2016;88:39—46.
[25] Sutter S, Nishiyama KK, Kepley A, Zhou B, Wang J, McMahon DJ, et al. Abnormalities in cortical bone, trabecular plates, and stiffness in postmenopausal women treated with glucocorticoids. J Clin Endocrinol Metab 2014;99:4231—40.